Study on Phase Transition and Crystallization Behavior of a Monotropic Liquid Crystalline Poly(ester−imide)

Sang Ouk Kim and In Jae Chung*

Department of Chemical Engineering, Korea Advanced Institute of Science and Technology, 373-1 Kusong, Yusong, Taejon 305-701, Korea

Received April 12, 2000; Revised Manuscript Received July 10, 2000

ABSTRACT: A poly(ester−imide) was synthesized from *N*-(10-carboxydecanyl) trimellitic imide and methylhydroquinone diacetate via melt transesterification condensation. It was characterized through thermal analysis, optical microscopy, wide-angle X-ray diffraction, and oscillatory rheometry. The poly(ester−imide) showed a monotropic mesophase transition behavior. The mesophase was identified as a nematic one from a unique hysteresis of viscoelastic properties. The crystallization behaviors in the isotropic melt phase and nematic mesophase were compared. They showed the same crystal structure and Avrami exponent value for crystallization. But the crystallization velocity was faster in the nematic phase. The crystal grown from the nematic phase showed a higher melting temperature than that grown from the isotropic phase.

Introduction

The mesophases of thermotropic polymers are classified into enantiotropic and monotropic according to the stability of the mesophase.[1] Because an enantiotropic type mesophase is the most stable phase in certain temperature region, the characterization is relatively easy. But a monotropic mesophase is stable below the crystal melting temperature. Only when crystallization is bypassed below the mesophase to isotropic phase transition with adequate cooling rate is the metastable mesophase temporarily observable. Thus, it is difficult to identify a monotropic mesophase.[2]

Up to now, various monotropic liquid crystalline polymers have been reported, which include polyesters,[3−5] polyethers and copolyethers,[6,7] poly(ester−imide)s,[8,9] polyurethanes,[10−12] polycarbonates,[13] etc. The reason for the formation of monotropic mesophase was attributed to the decrease in rigidity, the linearity, the symmetry, and the low aspect ratio of mesogenic groups in molecular chain.[2] Various techniques such as thermal analysis, polarized light microscopy study, and wide-angle X-ray diffraction study (WAXD) have been utilized to characterize the monotropic mesophase.[14−19] The crystallization of polymers can be retarded below the melting temperature with a fast cooling rate. On the other hand, low ordered mesophase transitions follow nearly the equilibrium transition.[18,20] Thus, as the cooling rate increases in DSC, the crystallization peak moves toward a lower temperature, but the isotropic phase to mesophase transition peak is lowered a little. Monotropic polymers show typical nucleation and growth morphology during crystallization above the mesophase to isotropic phase transition temperature. But mesophase texture persists until the completion of crystallization below the mesophase to isotropic phase transition temperature. Despite such distinct features in thermal transition and texture evolution behaviors, it is recommended that WAXD experiments using different cooling rates are necessary to precisely judge the nature of the transition.[2]

* To whom all correspondence should be addressed. Tel +08(42)869-3916, Fax +08(42)869-3910, E-mail chung@cais.kaist.ac.kr.

As mentioned by some authors, a monotropic liquid crystalline polymer can be used as a good material to study the effect of mesophase on the crystallization.[2,13,18,21−24] There has been a few reports on this topic. According to the initial phase (mesophase or isotropic phase), the melting temperature,[13,25] crystal structure,[22] and Avrami exponent values[18,21] changed. A more general conclusion was that the crystallization rates were faster in mesophases.[2,13,22−24]

In this article, a poly(ester−imide), containing 10 methylene units, is synthesized. A monotropic mesophase transition behavior is verified with DSC, PLM, and rheometry. The crystallization in mesophase is compared with that in the isotropic phase.

Experimental Section

Materials. Trimellitic anhydride, 11-aminoundecanoic acid, and methylhydroquinone were purchased from Aldrich Chemical Co. The methods of the acetylation of methylhydroquinone and the synthesis of *N*-(10-carboxydecanyl) trimellitic imide were reported elsewhere.[26,27] The polymerization scheme was the same, too. The chemical structure of synthesized poly(ester−imide) and its 125 MHz ^{13}C NMR spectrum are shown in Figure 1. It has to be noted that the synthesized poly(ester−imide) has random copolymeric character due to the asymmetric chemical structure of *N*-(10-carboxydecanyl) trimellitic imide and methylhydroquinone diacetates. The inherent viscosity of poly(ester−imide) is 0.48 dL/g, measured at 20 °C in NMP solution with the concentration of 0.5 g/dL.

Measurements. The solution of 60 mg of poly(ester−imide)s in 600 μL of deuterated trifluoroacetic acid was used for the measurement of ^{13}C NMR (Bruker, AMX FT 500 MHz) spectra of poly(ester−imide)s. A polarized light microscope (PLM, A Leitz, model Laborlux 12 Pols) equipped with a Mettler FP-2 hot stage was used to observe the anisotropic texture of poly(ester−imide). Thermal transition and isothermal crystallization kinetics studies were carried out with du Pont 2010 thermal analyzer under a nitrogen atmosphere. Wide-angle X-ray diffractograms were obtained using a Rigaku X-ray generator (Cu Kα_1 radiation with $\lambda = 0.154\ 06$ nm). Film type samples were molded, controlling thermal histories. Temperature sweep measurements of viscoelastic properties were conducted with a rheometer (PHYSICA RheoLab MC 120). Parallel plate geometry was used for disk shape molded samples. Strain was fixed at 0.5%, which is the lowest value of the rheometer. There was no evidence of nonlinearity on

10.1021/ma000639n CCC: $19.00
Published on Web 09/07/2000

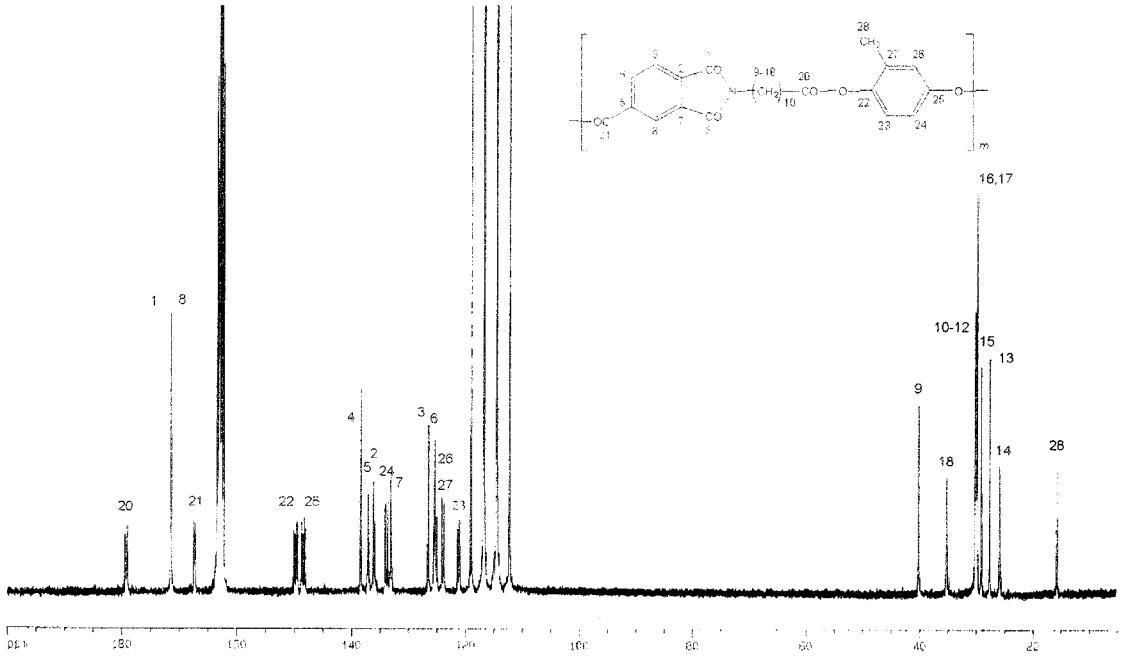

Figure 1. Chemical structure and 125 MHz ^{13}C NMR spectra of synthesized poly(ester−imide).

Table 1. Peak Temperatures and the Heats of All Thermal Transitions Recorded on DSC at Various Cooling Rates

cooling rate (°C/min)	T_1 (°C)	ΔH_1 (kJ/mru)	T_2 (°C)	ΔH_1 (kJ/mru)	T_3 (°C)	ΔH_1 (kJ/mru)	T_4 (°C)	ΔH_1 (kJ/mru)
0.5	118.3	5.2	112.0	5.9				
1	117.8	5.4	105.9	5.4	91.1	0.4		
3	116.6	5.4	102.5	2.1	85.86	2.5		
5	115. 6	5.4	101.3	1.7	82.63	2.9		
10	113.2	5.4	99.3	1.7	89.4	0.8	75.8	1.7

the deformation sweep measurements at various temperatures with the small value of strain. But it was impossible to check linearity below 100 °C, where the crystallization proceeded very fast.

Results and Discussion

Thermal Transition Behavior and Texture Evolution of Poly(ester−imide). Figure 2 shows the DSC cooling and heating curves of the synthesized poly(ester−imide). A glass transition temperature is observed around 47 °C on the heating curve with a rate of 10 °C/min and then followed by a weak exotherm around 89 °C and an endotherm around 147 °C. The scan rate of cooling was varied from 0.5 to 10 °C/min. At the cooling rate of 0.5 °C/min, a sharp and a broad exotherm are observed at high and low temperatures, respectively. As the cooling rate increases, the low-temperature exotherm split into two or three exotherms, and their peak positions shift to lower temperatures. However, the high-temperature exotherm keeps the same peak position and amount of heat, which is a typical feature of a low ordered mesophase transition.[18,20] Table 1 summarizes the peak temperatures and the amount of heat for all exothermic transitions measured on DSC cooling scans.

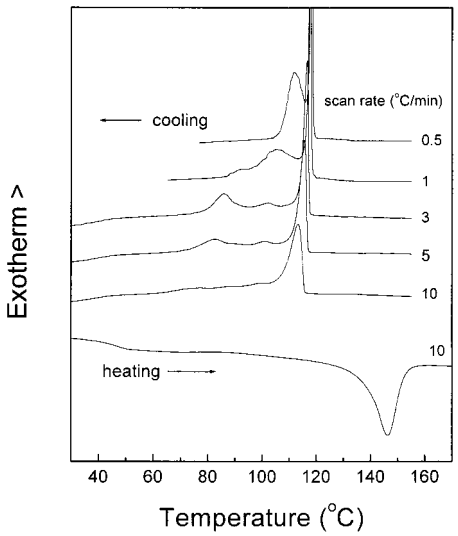

Figure 2. DSC cooling and heating curves of poly(ester−imide)s. The heating scan was performed after the 10 °C/min cooling scan.

Figure 3 shows sequential cooling and heating curves of DSC, measured to check a hidden endothermic transition. After cooling from isotropic melt at a rate of 10 °C/min, the samples were isothermally annealed at 100 °C for various times. And successive heating scans were conducted at the same rate of 10 °C/min. The heating curve without annealing has the same amount of heat as that of exotherm on cooling. As the annealing time increases, the low-temperature endotherm gets weaker and then disappears completely after 6 min. On the other hand, a high-temperature endotherm around 145 °C grows and reaches a constant value, which is consistent with the endotherm at 147 °C on heating curve shown in Figure 2.

The textures at various temperatures were observed by polarized light microscopy. Figure 4a shows the micrograph taken at 100 °C after cooling from an isotropic melt at a rate of 10 °C/min. The threadlike texture of mesophase is observed. Such a texture emerges around 115 °C during cooling, which agrees

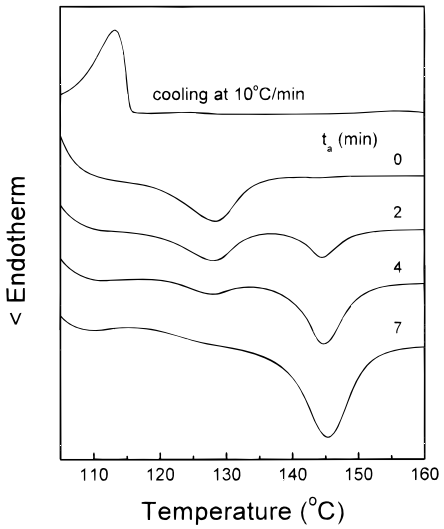

Figure 3. DSC heating curves of the poly(ester−imide)s, which was first cooled from isotropic melt at 10 °C/min and then annealed at 100 °C for various times.

with the highest temperature exotherm on DSC cooling curves in Figure 2. The texture evolution is all at once through the whole sample. The further annealing does not bring about any noticeable textural change. On the subsequent heating, the sample becomes isotropic around 145 °C. On the immediate reheating from 100 °C, the texture becomes isotropic around 125 °C. In contrast, when the annealing temperature was above 120 °C, the texture evolution is quite different. Figure 4b shows micrographs taken during isothermal annealing at 125 °C, which depicts typical nucleation and growth morphology of crystallization. After cooling to 125 °C from isotropic melt, the initial texture is isotropic. But as the annealing time increases, birefringent spots develop and grow. The growth rate is very slow compared with the threadlike texture formation. The crystal melts around 145 °C on reheating.

Phase Identification of a Poly(ester−imide) by a Rheological Method. It has been known that crystallization and mesophase transition show different rheological behavior. Both complex viscosity and storage modulus increase abruptly on crystallization and decrease again on subsequent melting. It is known as a hystereses of viscoelastic properties due to the supercooling of melt phase.[26−29] Viscosity and modulus increase in low ordered smectic formation too, but large hysteresis has not been observed.[29] The frequency dependence of moduli did not show a typical terminal slope in the smectic phase.[30−32] In the case of the nematic to isotropic (N−I) phase transition viscoelastic properties show distinct peak shapes due to the low-viscosity characteristic of the nematic phase.[26−29,33−38]

The temperature scans of complex viscosity and storage modulus are shown in Figure 5. The cooling scan was performed first and followed by the heating scan. Scan rates were 10 °C/min. The viscosity and the modulus show the typical peak shapes for the isotropic to nematic (I−N) transition during cooling in the temperature range of approximately 100−120 °C and then increase rapidly, converging to a high value. The peak in this temperature range corresponds to the high-temperature exotherm on DSC cooling curves in Figure 2. On the immediate heating the high viscoelastic values persist up to 120 °C. They start to decrease drastically at about 125 °C and meet the values of cooling scan

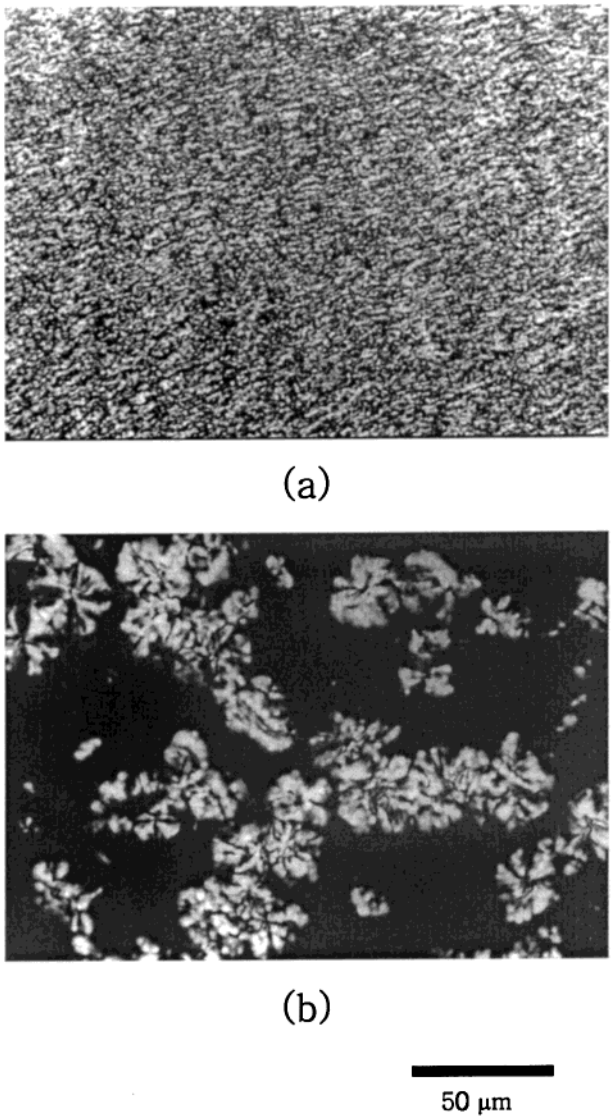

Figure 4. Polarized light micrographs of poly(ester−imide): (a) at 100 °C after cooling from isotropic melt with the rate of 10 °C/min; (b) isothermally annealed at 125 °C for 2 h after cooling from isotropic melt at the same rate. The crystal morphology showed positive optical sign on the quarter wave retardation plate test.

around 150 °C. The temperature at which viscoelastic properties increase abruptly on cooling matches with the temperature showing a minor exotherm observed on DSC cooling scan. And the temperature at which the viscoelastic properties decrease on heating matches with that of the melting endotherm on DSC heating scan. From the distinct hysteresis of viscoelastic properties, one can find that the polymer is a monotropic liquid crystalline polymer and that, moreover, the metastable mesophase is a nematic phase.

Figure 6 shows the cooling scans of viscoelastic properties at various cooling rates. The viscoelastic properties show peak shapes around the I−N transition on 3 °C/min cooling scan curves in Figure 6a, whereas the peak shape is partially obscured due to crystallization when the cooling rate is 1 °C/min in Figure 6b. At the cooling rate of 0.5 °C/min the peak shape is not seen anymore. Instead, the complex viscosity and storage modulus rapidly grow from approximately 110 °C (Figure 6c). Two exothermic transitions are discernible in DSC cooling curve at the cooling rate of 0.5 °C/min,

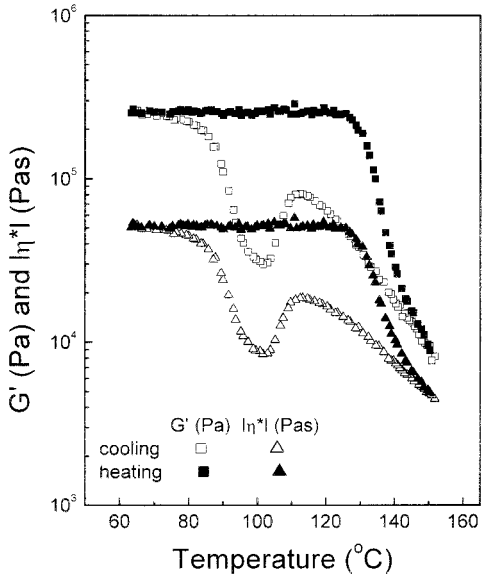

Figure 5. Cooling and immediate heating scans of storage modulus (G') and complex viscosity ($|\eta^*|$) at the scan rate of 10 °C/min. $\gamma = 0.5\%$, $\omega = 5$ rad/s.

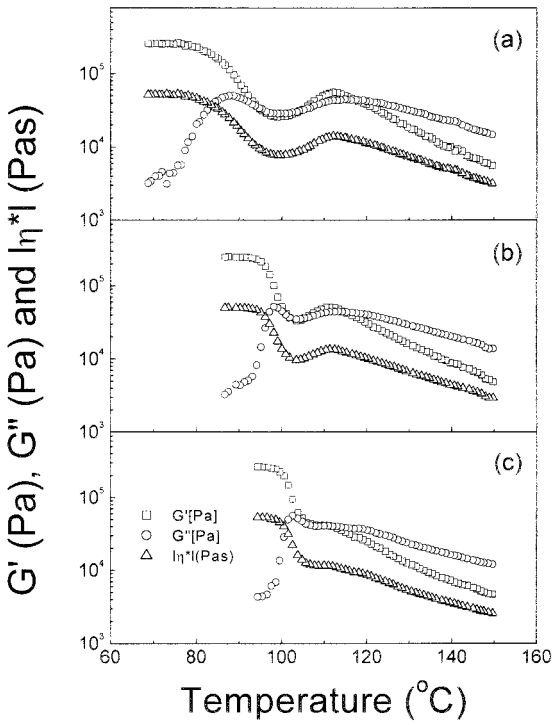

Figure 6. Cooling scans of storage modulus (G'), loss modulus (G''), and complex viscosity ($|\eta^*|$) at scan rate of (a) 3, (b) 1, and (c) 0.5 °C/min. $\gamma = 0.5\%$, $\omega = 5$ rad/s.

as shown in Figure 2. The discrepancy between rheological measurement and DSC might be attributed to the difference of the sample sizes of the instruments. Because the sample size of the rheometry is much larger than that of DSC, the wide temperature distribution can occur during temperature scan measurements.

From the moduli variations recorded on cooling, tan δ is plotted against temperature in Figure 7. The curve measured at 0.5 °C/min changes the shape of slope around 110 °C and then decreases abruptly due to crystallization. When the cooling rate is 1 °C/min, the tan δ curve shows a slope inversion from 110 °C, after which tan δ starts to decrease again from approximately

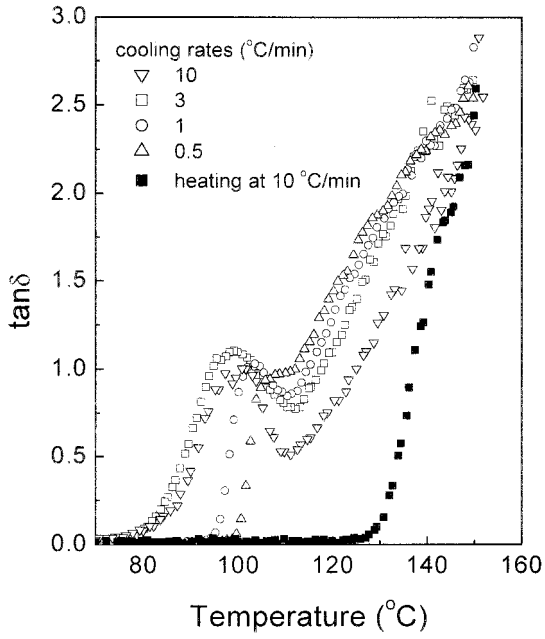

Figure 7. Cooling scans of tan δ at indicated scan rate. $\gamma = 0.5\%$, $\omega = 5$ rad/s.

100 °C. The second decrease in tan δ is due to the crystallization. The curves measured at 3 and 10 °C/min show the larger temperature range of slope inversion with the gentle shape, which is ascribed to the I−N phase transition rather than the crystallization. The slope inversion of the tan δ curve at the I−N transition was already reported by our group.[27]

Figure 8 shows the viscoelastic properties obtained during sequential scans of cooling, intermittent isothermal annealing, and heating scans. The scan methods are similar to those of DSC experiment shown in Figure 3. The immediate heating without annealing leads to the different peak shape from that on cooling in Figure 8a. As the isothermal annealing time increases, the peak shape on heating gets weaker and changes to a plateau, which extends up to the crystal melting transition, as shown in Figure 8d.

Crystallization Behaviors of Poly(ester−imide). As noted above, a monotropic liquid crystalline polymer can be used as a good example to investigate the effect of mesophase on crystallization behavior. At first, the equilibrium N−I phase transition temperature is obtained by extrapolating the peak temperature obtained on DSC cooling. The intercept at the cooling rate of zero turns out to be 119.7 °C. The crystallization behavior is checked around this transition temperature.

WAXD patterns were obtained for poly(ester−imide)s annealed around the equilibrium transition temperature. All samples were preheated above the melting temperature and then air quenched to each annealing temperature. The annealing time was given sufficiently long enough for the completion of crystallization. All annealed samples show almost the same patterns in Figure 9: one peak at middle angle and five peaks at wide angles. It means that the crystals developed from mesophase and isotropic phase have the same unit cell structure. The crystal structure is the same with that of the poly(ester−imide), made from *N*-(6-carboxyhexyl) trimellitic imide and methylhydroquinone diacetates.[27] The identical crystal structure may need an additional comparison of the crystallization behavior. In a earlier report by Pardey and co-workers[22] on monotropic liquid

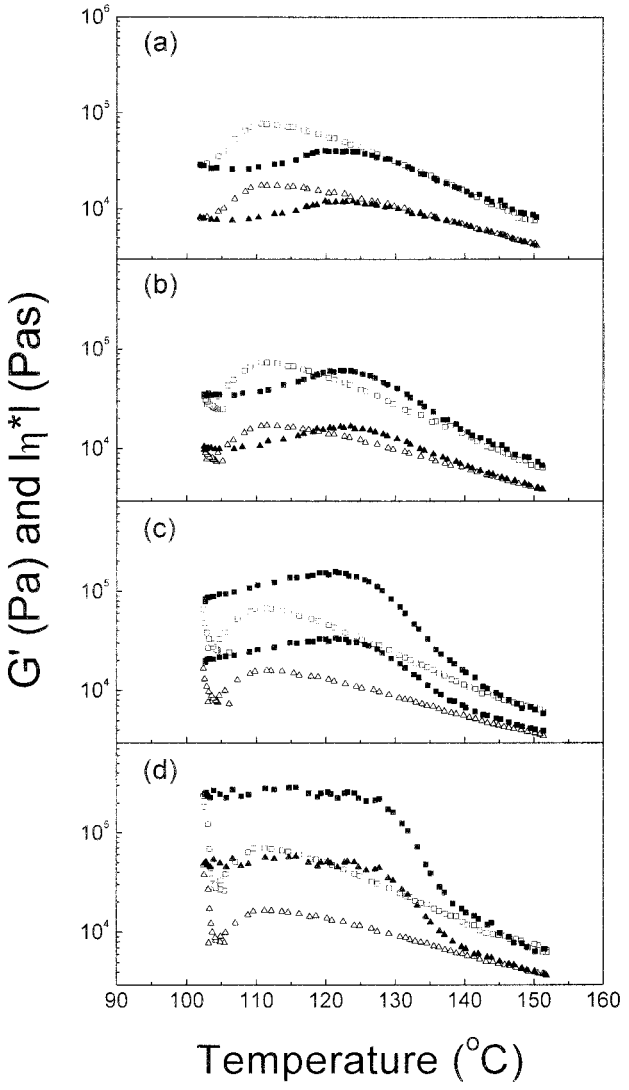

Figure 8. Cooling and subsequent heating scans of storage modulus (G') and complex viscosity ($|\eta^*|$) after isothermally annealed at 103 °C for (a) 0, (b) 5, (c) 7, and (d) 10 min. γ = 0.5%, ω = 5 rad/s. Open symbols stand for cooling scans and closed symbols for heating scans.

crystalline poly(ester−imide)s showing smectic phase, the poly(ester−imide)s containing an even number (except four) of methylene spacer showed different crystal structures according to the initial phase status, which was an interesting example that metastable state affected the structure of the ultimate stable state. The WAXD pattern of the sample, which was quenched in liquid nitrogen from isotropic melt, does not show any noticeable crystalline peaks. However, the sample was not transparent, which indicates a nematic phase.

The isothermal crystallization experiments were performed on DSC. Before each measurement DSC was preequilibrated at the annealing temperature. The sample pan, annealed at 160 °C for several minutes, was directly moved onto DSC, and the isothermal transition behaviors were recorded. After each isothermal experiment, the heating scan was performed at a rate of 5 °C/min. Figure 10 shows the isothermal curves measured at 116.2 and 119.1 °C, which are just below the equilibrium N−I phase transition temperature. There are two exothermic processes on each curve. The short time exotherms result from the I−N phase transition and the long time ones from crystallization. Similar behaviors

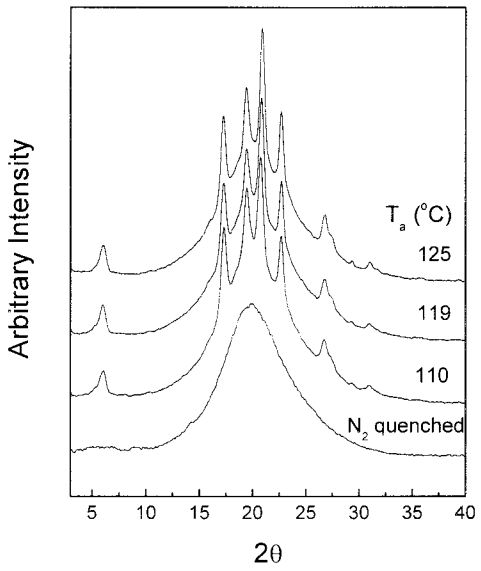

Figure 9. WAXD patterns for the poly(ester−imide), which is isothermally annealed at indicated temperature until the completion of crystallization or nitrogen quenched from isotropic melt.

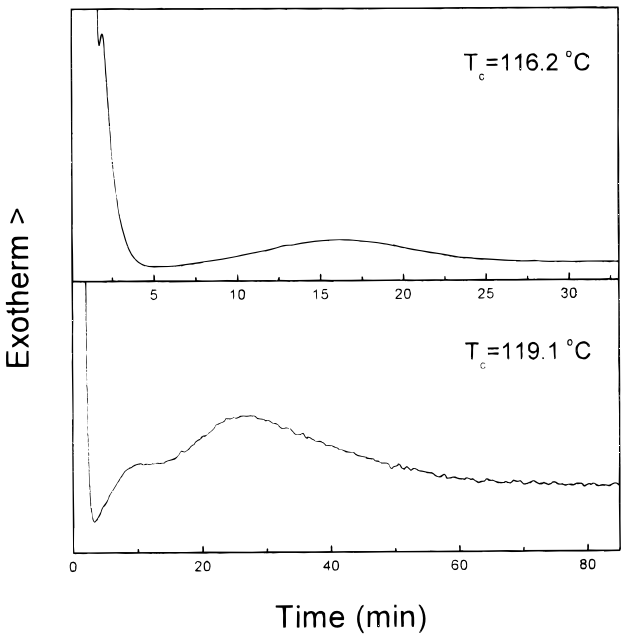

Figure 10. DSC isothermal curves recorded at 116.2 and 119.1 °C.

were reported for the monotropic liquid crystalline poly(ester−imide)s and polyethers.[18,22,25] Keller and coworkers[2,23] have described that just below the melting temperature of the metastable phase (I−N transition temperature in our case) the stable phase and metastable phase have same order of transition velocity. Below 116.2 °C and above the N−I transition temperature, the isothermal curves show only one exothermic process. During the annealing below 116.2 °C, the heat generated from isothermal crystallization is significantly lower than that of fusion on the heating scan after annealing. The difference of heat amount is approximately 5.4 kJ/mru, which is almost the same with the heat of the I−N phase transition. It implies that the nematic phase formation is formed completely before the thermal equilibration of DSC. In contrast, when the measurements are done above 119.1 °C, the

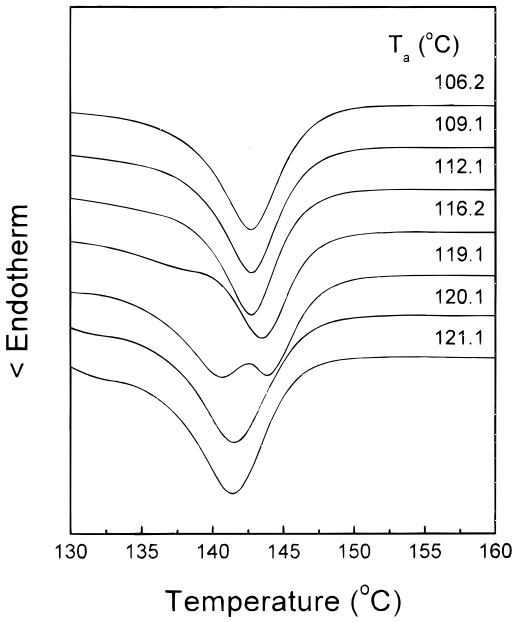

Figure 11. DSC heating curves recorded at 5 °C/min after isothermal annealing at various temperatures.

heat of crystallization observed on isothermal annealing (approximately 7.9 kJ/mru) matches relatively well with the heat of fusion on the heating scan.

Figure 11 shows the DSC heating curves measured after the isothermal annealing at the various temperatures. The isothermal annealing from 106.2 to 112.1 °C leads to one melting endotherm. The peak temperature of the endotherm shifts slowly toward a higher temperature, as the annealing temperature becomes higher. A weak shoulder emerges at around 138 °C when the sample is annealed isothermally at 116.2 °C. And the major peak at the high temperature shifts abruptly to a high temperature. The weak shoulder grows to be a major one, when the sample is annealed at 119.1 °C. Only the low-temperature endotherm develops above the N−I phase transition temperature (120.1 and 121.1 °C), and it shifts toward a higher temperature with annealing temperature again. As shown in Figure 10, nematic phase formation is relatively slower at 116.2 and 119.2 °C. In addition, liquid crystalline polymers, prepared from condensation reaction, might have a relatively broad biphasic region due to their polydispersity.[39] On the backgrounds the dual endotherms can be assigned. The high-temperature endotherm is the melting of the crystal grown in nematic phase, and the low-temperature one corresponds to that in isotropic phase. Similar behaviors have been reported for various monotropic liquid crystalline polymers.[13,24,25] Cheng and co-workers[13,24] discussed that the nematic phase acted as a nucleus for crystallization.

The isothermal crystallization can be interpreted with the Avrami equation

$$\theta = 1 - \exp(-kt^n) \qquad \theta = \frac{\Delta H(t)}{\Delta H_{\text{total}}}$$

where k is a temperature-dependent rate constant and n is the dimension of nucleation and crystal growth. θ is the transform fraction at time t. ΔH_{total} is the total enthalpy of exotherm at each temperature, and $\Delta H(t)$ is the enthalpy of transform progressed until time t.

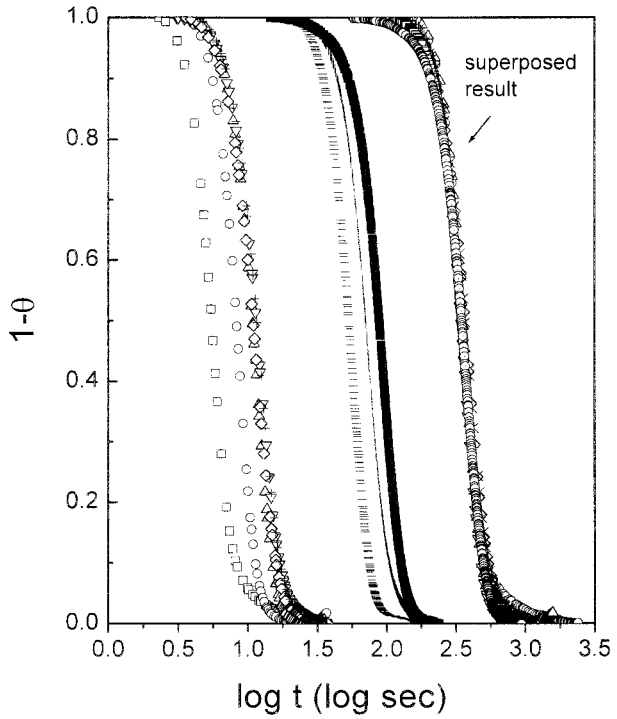

Figure 12. Extent of crystallization vs log time curves at various temperatures: □, 96.1 °C; ○, 99.1 °C; △, 102.1 °C; ▽, 106.1 °C; ×, 109.2 °C; +, 112.1 °C; −, 120.1 °C; |, 121.1 °C; ■, 122.1 °C and superposed result.

The isotherms obtained on DSC are converted to the degrees of crystallization by integrating the isothermal curves with time. Figure 12 shows the degrees of crystallization in the temperature range from 96. 1 to 122.2 °C. The crystallization velocity is too fast to obtain reasonable exotherm below and too slow above the range. All curves show similar shape when plotted with log time scale regardless of crystallization temperature. When all curves are shifted with log time axis, they superpose on a single line. Such superposition implies that all measured curves have the same Avrami exponent value.

Figure 13 shows the Avrami plots. The slopes of the all curves are around four. It is a surprising result that the crystallizations in isotropic and nematic phases show the same dimension. Different values of the Avrami exponent have been reported on a monotropic polyurethane and poly(ester−imide)s.[18,21] In the polarized light micrographs of poly(ester−imide) shown in Figure 4b, one can find that the size of the spherulite is diverse, which means a thermal nucleation. Therefore, the crystal growth in the isotropic phase can be considered as approximately three-dimensional. In contrast, the nucleation and crystal growth dimension in nematic phase are indiscernible due to the anisotropy of mesophase. Usually liquid crystalline polymers do not exhibit a distinct morphological change during crystallization in the mesophase. The restraints make it hard to discuss the crystallization mechanism in the mesophase.

The crystallization velocity at a certain temperature can be demonstrated by measuring the time to reach some conversion of crystallization. The time for half-conversion is plotted with temperature in Figure 14. It is less than 15 min in the mesophase but increases rapidly in the isotropic phase. It is more than 80 min even at 2.4 °C above the N−I transition temperature.

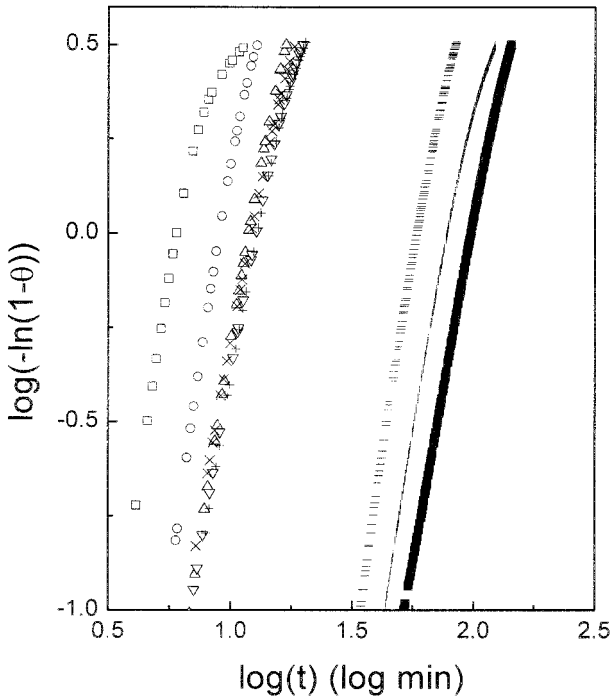

Figure 13. Avrami plots at various temperatures. Symbols are the same as in Figure 12.

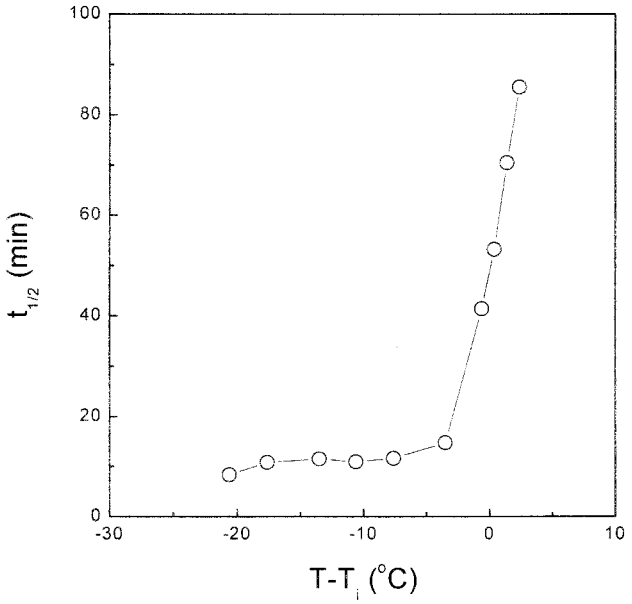

Figure 14. The time to reach half conversion of crystallization at various temperatures. Temperature is normalized by subtracting the equilibrium N−I transition temperature.

The acceleration of crystallization in mesophase has been reported for various monotropic liquid crystalline polymers.[2,20−23] The difference of crystallization rate may originate from the change of nucleation rate or crystal growth rate or both of them. However, as noted above, it has been reported that liquid crystalline polymers do not show distinct morphology change during crystallization, the same with our cases. There have been very few exceptional cases in liquid crystalline polymers which show spherulitic crystal morphology in the mesophase. They are well-known series of semiflexible polyethers synthesized by Percec and coworkers,[40,41] whose mesophase formation were based on conformational isomerism. For a series of polyethers containing odd number of methylene spacers Yandrasits and co-workers[25] observed spherulites in nematic phase under polarized light microscopy. Heberer and coworkers[23] observed similar morphology evolution for another polyether. They observed that both nucleation and growth rates were faster in nematic phase. However, neither nucleation rate nor crystal growth rate showed discontinuity at the N−I transition temperature, which was contrary to the overall crystallization rate. They concluded that the spherulites did not grow from the whole sample but from the isotropic portion included in the mesophase.

Conclusion

A poly(ester−imide) was synthesized from *N*-(10-carboxydecanyl) trimellitiimide and methylhydroquinone diacetate. The chemical structure was confirmed with ^{13}C NMR spectroscopy measurements. Upon DSC cooling scan a major exothermic transition was almost independent of scan rate. It occurred at a temperature far below the endothermic transition on heating scan. The poly(ester−imide) showed a threadlike texture of the mesophase when cooled below the endothermic transition but spherulitic crystal growth when annealed above the transition. The modulus and viscosity showed a peak shape at the transition during cooling, which was a clear evidence of monotropic type nematic mesophase formation. The crystallization behaviors in the nematic phase were compared with that in the isotropic phase. The crystal structure did not vary with initial phase status despite the clear morphological distinction observed on polarized light microscopy. The Avrami kinetics experiment led to the exponent value of four for the crystallization in both phases. The crystallization was faster in the mesophase than that in isotropic phase, which was consistent with the results of other monotropic liquid crystalline polymers. When the samples were annealed isothermally just below the N−I phase transition temperature, dual endotherms were observed. The high-temperature endotherm was assigned to the melting of the crystal formed in nematic phase and the low-temperature one to that of the crystal formed in the isotropic phase.

Acknowledgment. This work was financially supported by the Korea Science and Engineering Foundation (KOSEF) under Contract 971-0804-039-2.

References and Notes

(1) Percec, V.; Keller, A. *Macromolecules* **1990**, *23*, 4347−4530.
(2) (a) Keller, A.; Cheng, S. Z. D. *Polymer* **1998**, *39*, 4461−4487. (b) Cheng, S. Z. D.; Keller, A. *Annu. Rev. Mater. Sci.* **1998**, *28*, 533−562.
(3) Zhou, Q. F.; Duan, X. Q.; Liu, Y. L. *Macromolecules* **1986**, *19*, 247−249.
(4) Fujishiro, K.; Lenz, R. W. *Macromolecules* **1992**, *25*, 81−87.
(5) Bashir, Z.; Khan, N. *J. Polym. Sci., Polym. Phys.* **1996**, *34*, 2077−2084.
(6) Percec, V.; Yourd, R. *Macromolecules* **1989**, *22*, 524−537.
(7) Percec, V.; Yourd, R. *Makromol. Chem.* **1996**, *191*, 25−48.
(8) Adduci, J. M.; Facinelli, J. V.; Lenz, R. W. *J. Polym. Sci., Polym. Chem.* **1994**, *32*, 2931−2936.
(9) Kricheldorf, H. R.; Probst, N.; Schwarz, G.; Wutz, C. *Macromolecules* **1996**, *29*, 4234−4240.
(10) Papadimitrakopoulos, F.; Hsu, S. L.; MacKnight, W. J. *Macromolecules* **1992**, *25*, 4671−4681.
(11) Lee, J. B.; Kato, T.; Uryu, T. *Polym. J.* **1995**, *27*, 664−672.
(12) Lee, J. B.; Kato, T.; Ujiie, S.; Iimura, K.; Uryu, T. *Macromolecules* **1995**, *28*, 2165−2171.
(13) Cheng, Y. Y.; Cebe, P.; Schreuder-Gibson, H.; Bluhm, A.; Yeomans, W. *Macromolecules* **1994**, *27*, 5440−5448.

(14) Ungar, G.; Feijoo, J. L.; Keller, A.; Yourd, R.; Percec, V. *Macromolecules* **1990**, *23*, 3411−3416.
(15) Cheng, S. Z. D.; Yandrasits, M. A.; Percec, V. *Polymer* **1991**, *32*, 1284−1292.
(16) Yandraists, M. A.; Cheng, S. Z. D.; Zhang, A.; Cheng, J.; Wunderlich, B.; Percec, V. *Macromolecules* **1992**, *25*, 2112−2121.
(17) Papadimitrakopoulos, F.; Hsu, S. L.; MacKnight, W. J. *Macromolecules* **1992**, *25*, 4682−4691.
(18) Pardey, R.; Zhang, A.; Gabori, P. A.; Harris, F. W.; Cheng, S. Z. D.; Adduci, J.; Facinelli, J. V.; Lenz, F. W. *Macromolecules* **1992**, *25*, 5060−5068.
(19) Pardey, R.; Shen, D.; Gabori, P. A.; Harris, F. W.; Cheng, S. Z. D.; Adduci, J.; Facinelli, J. V.; Lenz, R. W. *Macromolecules* **1993**, *26*, 3687−3697.
(20) Ge, J. J.; Zhang, A.; McCreight, K. W.; Ho, R. M.; Wang, S. Y.; Jin, X.; Harris, F. W.; Cheng, S. Z. D. *Macromolecules* **1997**, *30*, 6498−6506.
(21) Smyth, G.; Valles, E. M.; Pollack, S. K.; Grebowicz, J.; Stenhouse, P. J.; Hsu, S. L.; MacKnight, W. J. *Macromolecules* **1990**, *23*, 3389−3398.
(22) Pardey, R.; Wu, S. S.; Chen, J.; Harris, F. W.; Cheng, S. Z. D.; Keller, A.; Aducci, J.; Facinelli, J. V.; Lenz, R. W. *Macromolecules* **1994**, *27*, 5794−5802.
(23) Heberer, D.; Keller, A.; Percec, V. *J. Polym. Sci., Polym. Phys.* **1995**, *33*, 1877−1894.
(24) Cheng, Y.; Cebe, P.; Capel, M.; Schreuder-Gibson, H.; Bluhm, A. *J. Polym. Sci., Polym. Phys.* **1995**, *33*, 2331−2341.
(25) Yandrasits, M. A.; Chen, J.; Arnold, F. E., Jr.; Cheng, S. Z. D.; Percec, V. *Polym. Adv. Technol.* **1994**, *5*, 775−784.
(26) Kim, T. K.; Kim, S. O.; Chung, I. J. *Polym. Adv. Technol.* **1996**, *8*, 305−318.
(27) Kim, S. O.; Kim, T. K.; Chung, I. J. *Polymer* **2000**, *41*, 4707−4717.
(28) Kim, T. K.; Kim, K. M.; Chung, I. J. *Polym. J.* **1997**, *29*, 85−94.
(29) Kalika, D. S.; Shen, M. R.; Yu, X. M.; Denn, M. M.; Iannelli, P.; Masciocchi, N.; Yoon, D. Y.; Parrish, W.; Friedrich, C.; Noel, C. *Macromolecules* **1990**, *23*, 5192−5200.
(30) Larson, R. G.; Winey, K. I.; Patel, S. S.; Watanabe, H.; Bruinsma, R. *Rheol. Acta* **1993**, *32*, 245−253.
(31) Hudson, S. D.; Lovinger, A. J.; Larson, R. G.; Davis, D. D.; Garay, R. O.; Fujishiro, K. *Macromolecules* **1993**, *26*, 5643−5650.
(32) Alt, D. J.; Hudson, S. D.; Garay, R. O.; Fujishiro, K. *Macromolecules* **1995**, *28*, 1575−1579.
(33) Wunder, S. L.; Ramachandran, S.; Gochanour, C. R. Weinberg, M. *Macromolecules* **1986**, *19*, 1696−1702.
(34) Blumstein, A.; Thomas, O.; Kumar, S. *J. Polym. Sci., Polym. Phys.* **1986**, *24*, 27−38.
(35) Kim, S. S.; Han, C. D. *Polymer* **1994**, *35*, 93−103.
(36) Chang, S.; Han, C. D. *Macromolecules* **1997**, *30*, 1656−1669.
(37) Chang, S.; Han, C. D. *Macromolecules* **1997**, *30*, 2021−2034.
(38) Gillmor, J. R.; Colby, R. H.; Hall, E.; Ober, C. K. *J. Rheol.* **1994**, *38*, 1623−1638.
(39) Nakai, A.; Wang, W.; Hashimoto, T.; Blumstein, A.; Maeda, Y. *Macromolecules* **1994**, *27*, 6963−6972.
(40) Percec, V.; Yourd, R. *Macromolecules* **1989**, *22*, 524−537.
(41) Percec, V.; Zuber, M. *Macromolecules* **1992**, *30*, 997−1016.

MA000639N